



Effect of projectile breakup in the system $^{19}\text{F} + ^{154}\text{Sm}$

Amritraj Mahato^a, Pankaj K Giri^a, D Singh^{a*}, Nitin Sharma^a, Sneha B Linda^a, Harish Kumar^b, Suhail A Tali^b, Nabendu K Deb^c, M Afzal Ansari^b, R Kumar^d, S Muralithar^d & R P Singh^d

^aDepartment of Physics, Central University of Jharkhand, Ranchi 835 205, India

^bDepartment of Physics, Aligarh Muslim University, Aligarh 202 002, India

^cDepartment of Physics, Gauhati University, Guwahati 781 014, India

^dInter University Accelerator Centre, Aruna Asaf Ali Marg, New Delhi 110 067, India

Received 4 May 2020

An attempt was made to understand the role of various entrance channel parameters on incomplete fusion dynamics by the measurements of excitation functions of evaporation residues populated via complete and incomplete fusion dynamics in the system $^{19}\text{F} + ^{154}\text{Sm}$ at projectile energy $\approx 4\text{-}6$ MeV/A. The stacked foil activation technique followed by offline gamma ray spectrometry was employed in these measurements. The measured excitation functions of various evaporation residues populated have been analyzed within the framework of statistical model code PACE-4. It has been observed that the measured excitation functions of xn and pxn emission channels agree well with the theoretical predictions of PACE-4. On the other hand, the measured excitation functions of α -emission channels have been found significantly enhanced over their theoretical predictions. This enhancement may be attributed to the incomplete fusion of the projectile ^{19}F as the calculations for incomplete fusion are not included in statistical model calculations. The incomplete fusion fraction has been deduced from the present measurements. Further, a systematic study has also been performed, which shows that the incomplete fusion increases significantly with entrance channel mass asymmetry at low projectile energy, differently for different projectiles.

Keywords: Excitation functions, Stacked foil activation technique, Complete and incomplete fusion, Incomplete fusion fraction, Entrance channel mass asymmetry

1 Introduction

The study of heavy ion induced nuclear reactions has been a subject of great interest for both experimental and theoretical nuclear physicists. Various nuclear fusion processes may take place in the collisions of heavy ions at projectile energy above the coulomb barrier. At projectile energies above coulomb barrier and below ≈ 10 MeV/nucleon, the complete fusion (CF) is supposed to be the dominant mode of nuclear reaction. However, a large fraction of incomplete fusion (ICF) has also been observed at these energies. In the complete fusion (CF) process, entire projectile fuses with the target and leads to the formation of highly excited compound nucleus, which further decays by evaporating light particles (neutrons, protons and α -particles) at the equilibrium stage. On the other hand, in case of ICF reactions, only a part of the projectile fuses with the target nucleus, leading to fractional transfer of momentum from the projectile to the target nucleus, while the remainder (generally α -particle) moves in the forward

direction as spectator. Britt and Quinton¹ observed the first experimental evidence of ICF in the break-up of projectiles like ^{12}C , ^{14}N , and ^{16}O into α -clusters. Further, a pioneer work in the understanding of ICF dynamics was done by Inamura *et al.*² through the charged particle- γ coincidence measurements for $^{14}\text{N} + ^{159}\text{Tb}$ system at beam energy about ≈ 7 MeV/A. Apart from experimental studies, several theoretical models have also been proposed to explain the characteristic features of ICF dynamics. Some of the most widely used models to explain ICF data are the breakup fusion model³, sum rule model⁴, promptly emitted particles model⁵, and exciton model⁶. These theoretical models can satisfactorily predict the contribution of ICF in some cases at projectile energy greater than 10 MeV/A. But none of these models can satisfactorily explain the gross features of ICF data at low projectile energy below 7 MeV/A. Hence, a clear understanding of the mechanism of ICF dynamics has yet to be established at low projectile energy. This makes the study of ICF dynamics still a relevant area of investigation. The contribution of low energy ICF reactions and their dependence on various entrance

*Corresponding author (E-mail: dsinghcuj@gmail.com)

channel parameters have been studied during the last few decades. Morgenstern *et al.*⁷ have observed the dependence of ICF dynamics on entrance channel mass asymmetry at relatively higher energies greater than 10 MeV/A. Recently, several investigators have shown great interest to study the dependence of ICF dynamics on various entrance channel parameters⁸⁻¹¹. Their studies show that the onset of ICF dynamics does not depend on a single entrance channel parameter, while it depends on various entrance channel parameters.

The present work has been carried out with a motivation to understand the dependence of ICF dynamics on various entrance channel parameters. The excitation functions (EFs) of evaporation residues (ERs) populated in $^{19}\text{F} + ^{154}\text{Sm}$ system at projectile energy range $\approx 4\text{-}6$ MeV/A have been measured and analyzed within the framework of statistical model code PACE-4¹².

2 Experimental Details

The present experiment was performed at Inter University Accelerator Centre (IUAC), New Delhi, India by using the 15UD Pelletron accelerator facility. The stacked foil activation technique followed by offline γ -ray spectroscopy was adopted for the present measurements. The isotopically enriched ^{154}Sm (enrichment = 98.69 %) targets of thickness $\approx 0.1\text{-}0.6$ mg/cm² were prepared by vacuum evaporation technique in the target preparation laboratory of IUAC, New Delhi. The ^{154}Sm enriched targets were deposited on aluminum (Al) –backings of thickness $\approx 1.0\text{-}1.5$ mg/cm². The Al-backings were used as catcher foil and energy degrader to trap the recoiling evaporation residues (ERs) during the irradiations. The thickness of each target and Al-backing foil was measured by weighing method using microbalance as well as using α -transmission method, which is based on the measurement of energy loss by 5.487 MeV α -particles from standard ^{241}Am source. The targets pasted on Al-catchers were cut into size of 1.2×1.2 cm² and pasted on stainless steel (SS) holders having concentric hole of 1.0 cm diameter. The irradiation was carried out in the General Purpose Scattering Chamber (GPSC) at IUAC, New Delhi. This chamber has an in-vacuum transfer facility (IVTF), which was used to minimize the time lapse between the stop of irradiations and start of the counting. A stack consisting of six ^{154}Sm targets along with Al-catchers was bombarded with energetic ^{19}F beam of energy

110 MeV. The beam current was monitored $\approx 2\text{-}4$ pA during the irradiation. The targets along with Al-catchers were placed normally to the beam direction so that the recoiling ERs may be trapped in the catcher foils of suitable thickness. The irradiation was carried out for ≈ 8 h, keeping in view the half-lives of interest. The beam flux was calculated by the total charge collected in the Faraday cup, placed behind the target-catcher foil assembly. After the irradiation, the stack of ^{154}Sm targets along with Al-catchers was taken out from the GPSC. The activities produced in each foil was then recorded using pre-calibrated high resolution high purity Germanium (HPGe) detector coupled to PC through CAMAC based CANDLE software¹³. Various standard γ -ray sources of known strength *viz.* ^{152}Eu , ^{60}Co etc. were used for the energy and efficiency calibration of the HPGe detector. The standard γ -ray sources and the irradiated samples were counted in same geometry to keep the geometry dependent detector efficiency same. The γ -ray spectra of individual target-catcher assembly were recorded at increasing time intervals. The populated ERs were identified on the basis of their characteristic γ -rays recorded in the spectrum and also by their decay curve analysis. The spectroscopic properties of ERs such as characteristic γ -ray energy, branching ratios and half-lives have been taken from literature^{14,15}. The production cross-section for different ERs has been determined using the standard formulation given in literature¹⁶. Several factors which may produce the errors and uncertainties in the measured cross-sections of the ERs and other experimental details are described in our earlier work⁸. The overall uncertainty from all factors was estimated to be less than 15 %.

3 Results and Discussion

In the present work, the excitation functions (EFs) of several ERs populated via xn, pxn, and α xn emission channels in the $^{19}\text{F} + ^{154}\text{Sm}$ system were measured. The measured EFs of these ERs were compared with the theoretical predictions of statistical model code PACE-4¹² to understand the involved reaction mechanism. The statistical model code PACE-4 is a Monte Carlo simulation code based on Hauser-Feshbach formalism¹⁷ used for the determination of the decay sequence of an excited compound nucleus (CN). The level density parameter 'a' ($= A/K$) MeV⁻¹, is one of the most important parameter in this code, where 'A' is the mass number of the compound nucleus and 'K' is called level

density parameter constant, which affects the equilibrium components. Most of the required input parameters have been used as default except the mass and charge of the projectile and target nucleus. More details about the analysis of measured excitation functions within the framework of PACE-4 code are given in our earlier work⁸. In the present analysis, it was observed that the measured cross sections of the ERs populated via xn and pxn emission channels were in good agreement with the PACE-4 predictions at level density parameter ($a = A / 10 \text{ MeV}^{-1}$), which indicates that these ERs are populated via CF process. As a representative case, the measured cross-sections of the ERs ^{167,168}Lu populated via xn (x= 5, 6) emission channels have been plotted along with PACE-4 predictions as a function of projectile energy and displayed in Fig. 1. It can be seen clearly in this figure that the measured cross-sections of these ERs are satisfactorily reproduced by the theoretical predictions of PACE-4 code at level density parameter constant $K=10$. These results indicate that the ERs ^{167,168}Lu are populated through only CF dynamics. Further, the measured cross-sections of ERs ^{165,166}Tm produced through α - emission channels in the system ¹⁹F + ¹⁵⁴Sm were plotted along with their theoretical predictions of PACE-4 and displayed in Fig. 2. It has been found during the decay curve analysis of ER ¹⁶⁵Tm that it is strongly fed from its higher charge precursor ¹⁶⁵Yb. The half life of the precursor ¹⁶⁵Yb ($T_{1/2} = 9.9 \text{ min}$) is quite smaller than that of the daughter ¹⁶⁵Tm ($T_{1/2} = 30.06 \text{ h}$). The independent production cross sections (σ_{indp}) of ER ¹⁶⁵Tm have been extracted from its measured cumulative cross sections (σ_{cumt}) using the formulation suggested by Cavinato *et al.*¹⁸ given as:

$$\sigma_{indp} = \sigma_{cumt} - F_{pre}\sigma_{pre} \quad \dots (1)$$

where F_{pre} is the precursor coefficient which is related with the branching ratio of precursor decay (P_{pre}) to the daughter nucleus as:

$$F_{pre} = P_{pre} \frac{T_{1/2}^D}{T_{1/2}^D - T_{1/2}^{pre}} \quad \dots (2)$$

Here $T_{1/2}^D$ and $T_{1/2}^{pre}$ are the half lives of daughter and precursor nuclei, respectively. In the present case of ER ¹⁶⁵Tm, the Eq. (1) reduces to the following form:

$$\sigma_{indp}(^{165}\text{Tm})\sigma_{cumt}(^{165}\text{Tm})1.0055\sigma_{pre}(^{165}\text{Yb}) \quad \dots (3)$$

The independent cross-sections (σ_{indp}) of ER ¹⁶⁵Tm have been plotted in Fig. 2(b). In case of ER ¹⁶⁵Tm, no precursor contribution was observed during the decay curve analysis. As can be observed from Fig. 2, the measured cross-sections are much enhanced over their theoretical values at higher projectile energy. Since ICF is not considered in PACE-4 calculations, this enhancement may be attributed to ICF of projectile ¹⁹F. The present results indicate that these ERs are populated not only by CF, but they have also a significant contribution from ICF of ¹⁹F, i.e., fusion of fragment ¹⁵N with the target ¹⁵⁴Sm (if ¹⁹F breaks up into α and ¹⁵N fragments). An attempt was made to estimate the ICF contribution

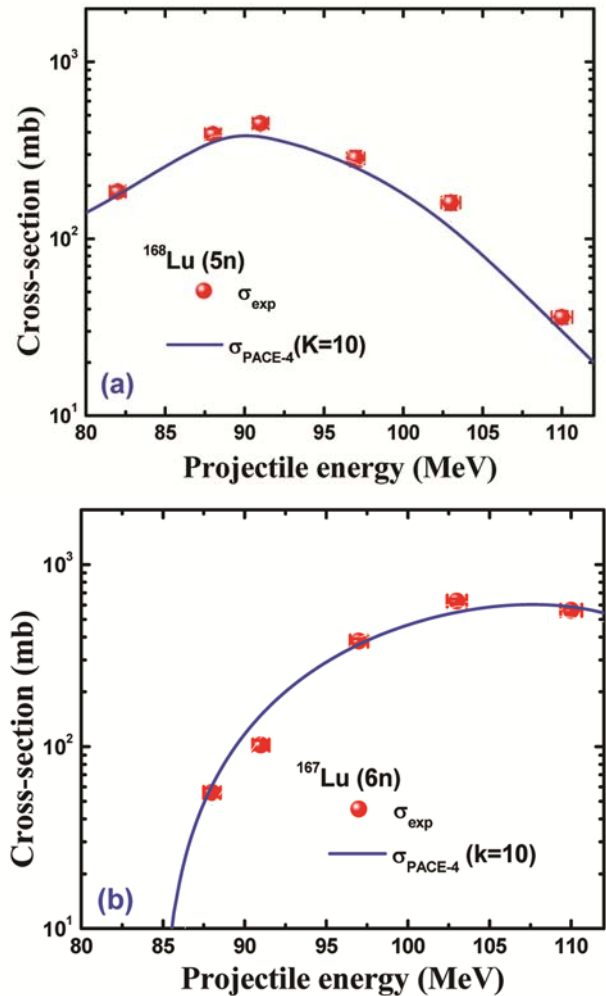


Fig. 1 — Measured cross-sections along with theoretical cross-sections (PACE-4) of evaporation residues ^{167,168}Lu populated through xn emission channels in ¹⁹F + ¹⁵⁴Sm system at energy $\approx 4\text{-}6 \text{ MeV/A}$.

from the measured excitation function data and to study the dependence of ICF dynamics on various entrance channel parameters. The ICF cross-sections for each identified ER were extracted as the difference between measured cross-sections and PACE-4 predictions. The total ICF cross-section of the system at a particular projectile energy was deduced by summing the ICF cross-sections of all measured ERs.

The ICF strength function (F_{ICF}) was also estimated for the present $^{19}\text{F} + ^{154}\text{Sm}$ system. The ICF strength function (F_{ICF}) is a measure of strength of ICF relative to total fusion (sum of CF and ICF cross-sections). This F_{ICF} fraction is defined as $F_{\text{ICF}}(\%) = (\sigma_{\text{ICF}}/\sigma_{\text{CF+ICF}}) \times 100$. The detailed description of determination of ICF fraction is given in our earlier work⁸. In the present measurements, some of the ERs could not be

measured due to their very long or short half-lives, low branching ratio, and stability, etc. As such, the deduced F_{ICF} should be treated as a lower limit of ICF contribution for the present system. The values of F_{ICF} have been taken at a constant value of factor $L_R = (\ell_{\text{max}} - \ell_{\text{crit}})/\ell_{\text{max}} = 0.096$, where ℓ_{max} and ℓ_{crit} are the maximum and critical angular momentum of the system, respectively, and their values were calculated using prescription⁴. The ICF fraction has been estimated from the presently measured EFs data for the system $^{19}\text{F} + ^{154}\text{Sm}$ and compared with those obtained for $^{16}\text{O} + ^{124}\text{Sn}$, $^{19}\text{O} + ^{103}\text{Rh}$, $^{20}\text{O} + ^{148}\text{Nd}$, $^{21}\text{O} + ^{93}\text{Nb}$, $^{22}\text{O} + ^{165}\text{Ho}$, $^{23}\text{O} + ^{20}\text{Ne} + ^{165}\text{Ho}$, $^{24}\text{O} + ^{59}\text{Co}$, $^{25}\text{O} + ^{55}\text{Mn}$, $^{26}\text{O} + ^{13}\text{C} + ^{175}\text{Lu}$, $^{27}\text{O} + ^{169}\text{Tm}$, $^{28}\text{O} + ^{159}\text{Tb}$, $^{29}\text{O} + ^{165}\text{Ho}$, $^{30}\text{O} + ^{12}\text{C} + ^{175}\text{Lu}$, $^{31}\text{O} + ^{159}\text{Tb}$, $^{32}\text{O} + ^{181}\text{Ta}$ systems at a constant value of $L_R = (\ell_{\text{max}} - \ell_{\text{crit}})/\ell_{\text{max}} = 0.096$. In earlier studies, Morgenstern *et al.*⁷ have shown that the ICF fraction generally increases linearly with entrance channel mass asymmetry of the system. With this in view, the deduced F_{ICF} values have been plotted as a function of entrance channel mass asymmetry and shown in Fig. 3. The solid curves are drawn to represent the incomplete fusion fraction (F_{ICF}) data for the different projectiles. This figure shows that the ICF fraction increases almost exponentially with the entrance channel mass asymmetry of the system, but differently for different projectiles. These present results indicate the effect of entrance channel mass asymmetry on ICF dynamics at projectile energy above the coulomb barrier. It is important to note that different slopes of F_{ICF} for different projectiles have been observed. This may be due to the fact that different projectiles have different breakup thresholds. Thus, present results clearly

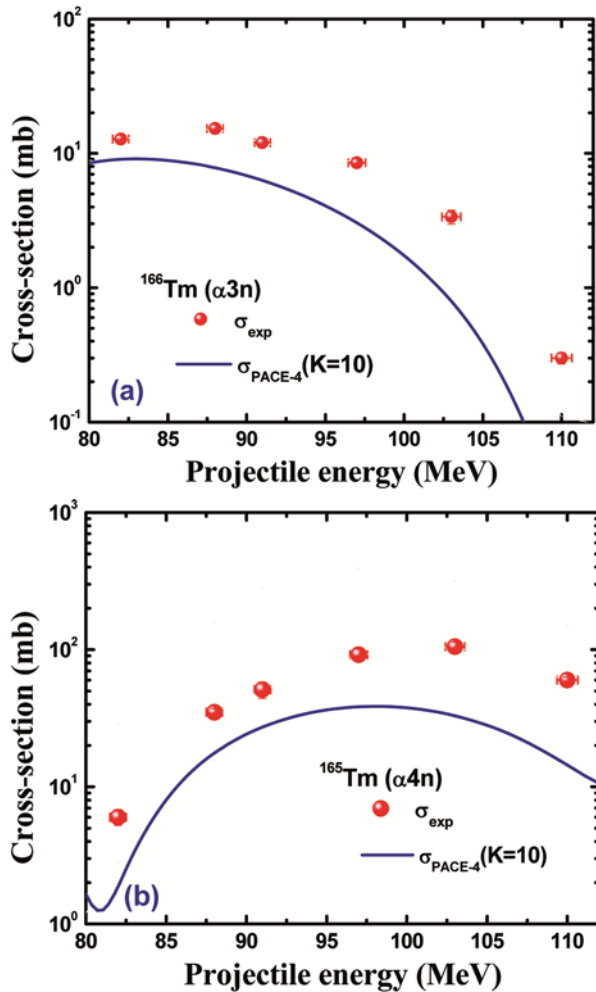


Fig. 2 — Sum of measured cross-sections along with theoretical cross-sections (PACE-4) of evaporation residues $^{165,166}\text{Tm}$ populated through α xn emission channels in $^{19}\text{F} + ^{154}\text{Sm}$ system at energy $\approx 4\text{-}6$ MeV/A.

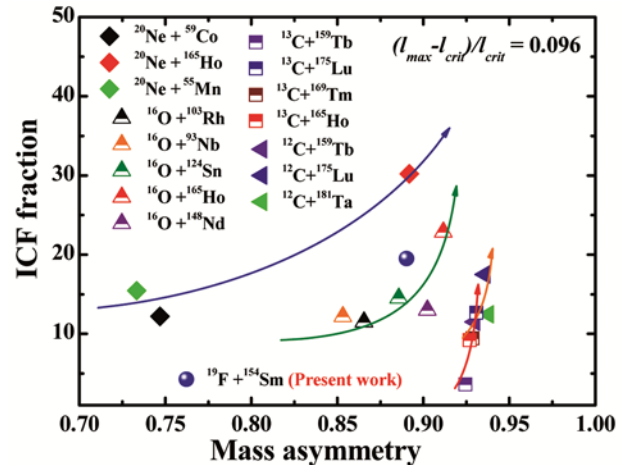


Fig. 3 — The incomplete fusion fraction (F_{ICF}) as a function of entrance channel mass asymmetry at a constant value of $L_R = (\ell_{\text{max}} - \ell_{\text{crit}})/\ell_{\text{max}} = 0.096$ for $^{19}\text{F} + ^{154}\text{Sm}$ system along with literature data²¹⁻³⁰.

highlight that the structure of projectile simultaneously affect the ICF dynamics along with other entrance channel parameters.

4 Summary and Conclusions

In the present work, excitation functions of evaporation residues populated via CF and ICF dynamics in the $^{19}\text{F} + ^{154}\text{Sm}$ system were measured in the energy range $\approx 4\text{-}6$ MeV/A. The measured EFs were analyzed within the framework of the statistical model code PACE-4, which provides CF only in its calculations. The measured EFs of evaporation residues populated through xn/pxn- emitting channels were found to be in good agreement with the predictions of PACE-4 code, indicating their production via CF only. On the other hand, the excitation functions of evaporation residues populated via α -emitting channels were found significantly enhanced over their theoretical predictions of PACE-4. This enhancement in the measured EFs was attributed to the population of these residues through ICF (i.e. breakup of projectile ^{19}F into $\alpha + ^{15}\text{N}$, followed by the fusion of one of the fragments with the target) in addition to CF process. It has been clearly observed that the breakup of non α -cluster projectile ^{19}F plays an important role along with CF at these low projectile energies. The dependence of ICF dynamics on entrance channel mass asymmetry for the present system along with some other systems taken from literature have also been studied. It was observed that the value of F_{ICF} increases almost exponentially with entrance channel mass asymmetry, independently for different projectiles. These results also indicate that the structure of projectile affects ICF dynamics along with other entrance channel parameters. The present study suggests that more systematic study regarding the influence of various entrance channel parameters on ICF dynamics using non α -cluster structured projectiles is required to get a complete understanding of these reactions at low projectile energy.

Acknowledgement

Authors express their thanks to Director and Convener, AUC, Inter University Accelerator Centre (IUAC), New Delhi, India, for providing all necessary facilities to perform the experiment. Authors are thankful to the target lab in-charge, Mr Abhilash S R and operational staff of pelletron, IUAC, New Delhi for their continuous support during the experiment. Authors are also thankful to Vice Chancellor of

Central University of Jharkhand (CUJ), Ranchi for the encouragement. Authors are indebted to the Head, Department of Physics, CUJ, Ranchi, for their motivation and support throughout the work. One of the authors DS acknowledges IUAC, New Delhi for providing financial support through research project (Ref. No. IUAC/XIII.3A/UFR/54321). AM thanks the UGC for providing financial assistance in the form of JRF (Ref. No- UGC/NET-JRF/520654).

References

- 1 Britt H C & Quinton A R, *Phys Rev*, 124 (1961) 877.
- 2 Inamura T, Kojima T, Nomura T, Sugitate T & Utsunomiya H, *Phys Lett B*, 84 (1979) 71.
- 3 Wilczynski J, Siwek-Wilczynska K, van Driel J, Gonggrijp S, Hageman D C J M, Janssens R V F, Lukasiak J & Siemssen R H, *Phys Rev Lett*, 45 (1980) 606.
- 4 Udagawa T & Tamura T, *Phys Rev Lett*, 45 (1980) 1311.
- 5 Bondroff J P, De J N, Fai G, Karvinen A O T & Randrup J, *Nucl Phys A*, 333 (1980) 285.
- 6 Blann M, *Phys Rev Lett*, 27 (1971) 337.
- 7 Morgenstern H, Bohlen W, Galster W, Grabisch K & Kyanowski A, *Phys Rev Lett*, 52 (1984) 1104.
- 8 Singh D, Ali R, Ansari M A, Tomar B S, Rashid M H, Guin R & Das S K, *Phys Rev C*, 83 (2011) 054604.
- 9 Kumar H, Tali S A, Ansari M A, Singh D, Ali R, Kumar K, Sathik N P M, Ali A, Parashari S, Dubey R, Bala I, Kumar R, Singh R P & Muralithar S, *Eur Phys J A*, 54 (2018) 47.
- 10 Singh D, Ali R, Afzal A M, Tomar B S, Rashid M H, Guin R, Das S K, Kumar R, Singh R P, Muralithar S & Bhowmik R K, *Pramana J Phys*, 82 (2014) 683.
- 11 Shuaib M, Sharma V R, Yadav A, Singh P P, Sharma M K, Singh D P, Kumar R, Singh R P, Muralithar S, Singh B P & Prasad R, *Phys Rev C*, 94 (2016) 014613.
- 12 Gavron A, *Phys Rev C*, 21 (1980) 230.
- 13 Kumar B P A, Subramaniam E T & Bhowmik R K, Conf Proc DAE SNP (Kolkata, 2001); URL: <http://www.iuac.res.in/NIAS/>.
- 14 Chu S Y F, Ekstrom L P & Firestone R B, The Lund/LBNL Nuclear Data Search (LBNL, Berkeley, CA, Version 2 0, 1999), <http://nucldata.nuclear.lu.se/toi/index.asp>
- 15 National Nuclear Data Centre, Brookhaven National Laboratory. <https://www.nndc.bnl.gov/chart/chartNuc.jsp>
- 16 Ansari M A, Singh R K Y, Sehgel M L, Mittal V K, Avasthi D K & Govil I M, *Ann Nucl Energy*, 11 (1984) 607.
- 17 Hauser W & Feshbach H, *Phys Rev*, 87 (1952) 366.
- 18 Cavinato M, Fabrici E, Gadioli E, Gadioli E E, Vergani P, Crippa M, Colombo G, Redaelli I & Ripamonti M, *Phys Rev C*, 52 (1995) 2577.
- 19 Singh D, Linda S B, Giri P K, Mahato A, Tripathi R, Kumar H, Tali S A, Parashari S, Ali A, Dubey R, Ansari M A, Kumar R, Muralithar S & Singh R P, *Phys Rev C*, 97 (2018) 064610.
- 20 Gupta U, Singh P P, Singh D P, Sharma M K, Yadav A, Kumar R, Singh B P & Prasad R, *Nucl Phys A*, 811 (2008) 77.
- 21 Giri P K, Mahato A, Singh D, Linda S B, Kumar H, Tali S A, Parasari S, Ali A, Ansari M A, Dubey R, Kumar R, Muralithar S & Singh R P, *Phys Rev C*, 100 (2019) 024621.

- 22 Sharma A, Kumar B B, Mukherjee S, Chakrabarty S, Tomar B S, Goswami A & Manohar S B, *J Phys G: Nucl Part Phys*, 25 (1999) 2289.
- 23 Kumar K, Ahmad T, Ali S, Rizvi I A, Agarwal A, Kumar R, Golda K S & Chaubey A K, *Phys Rev C*, 87 (2013) 044608.
- 24 Singh D, Ali R, Ansari M A, Rashid M H, Guin R & Das S K, *Nucl Phys A*, 879 (2012) 107.
- 25 Singh D, Giri P K, Mahato A, Linda S B, Kumar H, Ansari M A, Ali R, Tali S A, Rashid M H, Guin R & Das S K, *Nucl Phys A*, 981 (2019) 75.
- 26 Ali Rahbar, Singh D, Ansari M A, Rashid M H, Guin R & Das S K, *J Phys G: Nucl Part Phys*, 37 (2010) 115101.
- 27 Kumar H, Tali S A, Ansari M A, Singh D, Ali R, Kumar K, Sathik N P M, Parashari S, Ali A, Dubey R, Bala I, Kumar R, Singh R P & Muralithar S, *Nucl Phys A*, 960 (2017) 53.
- 28 Sharma V R, Yadav A, Singh P P, Singh D P, Gupta S, Sharma M K, Bala I, Kumar R, Muralithar S, Singh B P & Prasad R, *Phys Rev C*, 89 (2014) 024608.
- 29 Yadav A, Sharma V R, Singh P P, Singh D P, Sharma M K, Gupta U, Kumar R, Singh B P, Prasad R & Bhowmik R K, *Phys Rev C*, 85 (2012) 034614.
- 30 Tali S A, Kumar H, Ansari M A, Ali A, Singh D, Giri P K, Linda S B, Parashari S, Kumar R, Singh R P & Muralithar S, *Nucl Phys A*, 970 (2018) 208.
- 31 Yadav A, Sharma V R, Singh P P, Kumar R, Singh D P, Unnati, Sharma M K, Singh B P & Prasad R, *Phys Rev C*, 86 (2012) 014603.
- 32 Babu K S, Tripathi R, Sudarshan K, Shrivastava B D, Goswami A & Tomar B S, *J Phys G: Nucl Part Phys*, 29 (2003) 1011.